

Single-crystal sapphire resonator at millikelvin temperatures: Observation of thermal bistability in high- Q factor whispering gallery modes

Daniel L. Creedon,^{*} Michael E. Tobar, and Jean-Michel Le Floch

School of Physics (M013), University of Western Australia, 35 Stirling Hwy, Crawley, Western Australia 6009, Australia

Yarema Reshitnyk and Timothy Duty

School of Mathematics & Physics, University of Queensland, St. Lucia, Queensland 4072, Australia

(Received 3 September 2010; published 27 September 2010)

Resonance modes in single crystal sapphire (α -Al₂O₃) exhibit extremely high electrical and mechanical Q factors ($\approx 10^9$ at 4 K), which are important characteristics for electromechanical experiments at the quantum limit. We report the cool down of a bulk sapphire sample below superfluid liquid-helium temperature (1.6 K) to as low as 25 mK. The electromagnetic properties were characterized at microwave frequencies, and we report the observation of electromagnetically induced thermal bistability in whispering gallery modes due to the material T^3 dependence on thermal conductivity and the ultralow dielectric loss tangent. We identify “magic temperatures” between 80 and 2100 mK, the lowest ever measured, at which the onset of bistability is suppressed and the frequency-temperature dependence is annulled. These phenomena at low temperatures make sapphire suitable for quantum metrology and ultrastable clock applications, including the possible realization of the quantum-limited sapphire clock.

DOI: [10.1103/PhysRevB.82.104305](https://doi.org/10.1103/PhysRevB.82.104305)

PACS number(s): 42.65.Pc, 06.30.Ft, 42.60.Da, 76.30.-v

Experiments to couple superconducting qubits based on Josephson junctions to microwave resonators ($Q \approx 10^4$) at cryogenic temperatures have been well represented in recent scientific literature for a diverse range of circuit quantum electrodynamic applications. This includes generating nonclassical states of microwave cavities such as Fock states, where the limit on producing these nonclassical fields is due to the finite photon lifetime (or linewidth) of the resonator, as well as detecting a nanomechanical resonator at or near the ground state.¹⁻⁷ Sapphire resonators are of particular interest for future experiments due to their extremely low loss, with electronic Q factors of order 10^9 at 1.8 K,^{8,9} and mechanical Q factors as high as 5×10^8 at 4.2 K.^{10,11} The thermal, mechanical, and bulk electronic properties of sapphire have been characterized extensively over a wide range of temperatures from room temperature to superfluid liquid helium (1.6 K) using whispering-gallery (WG) mode techniques,^{12,13} but have never been examined in the regime approaching the absolute zero of temperature. Sapphire resonators at millikelvin temperature have the potential to play an important role in the next generation of quantum electronics and metrology experiments by virtue of this anomalously high Q factor. A significant body of research already exists in which sapphire has been used at cryogenic temperatures as a parametric transducer in an effort to reach the standard quantum limit.^{10,14-18} Oscillators can be prepared in their quantum ground state due to very low thermal phonon occupation when $T \ll hf/k_B$, where h and k_B are Planck's and Boltzmann's constants, respectively. For microwave oscillators such as those based on single-crystal sapphire resonators, the corresponding temperature regime is in the experimentally accessible millikelvin range, making them ideal candidates for quantum measurement experiments. It is thus important to characterize such devices in this unexplored ultralow temperature regime. In this paper we report on the measurements of the electromagnetic properties of a single-crystal sapphire

resonator at millikelvin temperature. The resonator used was a highest purity HEMEX-grade sapphire from Crystal Systems, similar to that used in several cryogenic sapphire oscillator (CSO) (Refs. 9, 19, and 20) and whispering-gallery maser oscillator (WHIGMO) experiments.²¹⁻²⁴ Here, we report on the observation of the lowest frequency-temperature turning points for WG mode resonances ever measured, as well as making the observation of a thermal bistability effect in sapphire for this ultralow-temperature regime. We give a model to predict thermal bistability threshold power and show that the effect is dependent on the thermal conductivity of the sapphire. Furthermore, we show that the bistability effect may be suppressed by operating at a “magic temperature,” where a frequency-temperature turning point occurs. Thus, combining the low-temperature operation with stabilization at a millikelvin frequency-temperature turning point gives the potential to realize a sapphire-based frequency standard at the quantum limit (rather than the thermal limit which has been previously reported²²).

The sapphire resonator, a cylinder 5 cm diameter \times 3 cm height, was cleaned in acid and mounted in a silver-plated copper cavity. The resonator is machined such that the anisotropy c axis of the sapphire is aligned with the cylindrical z axis. A radially oriented loop probe and axially oriented straight antenna were used to couple microwave radiation in and out of the crystal. The cavity was attached to the mixing chamber of a dilution refrigerator with a copper mount and cooled to 25 mK. The fundamental quasitransverse magnetic Whispering Gallery modes $WGH_{m,0,0}$, with azimuthal mode number m from 13 to 20, were characterized over a range of temperatures using a vector network analyzer. We observed that particularly high- Q WG modes exhibited a hysteretic behavior, which was thermal in nature. The frequency of the WG modes supported in the resonator are dependent on both the physical dimensions of the crystal and its permittivity, the latter effect being more than an order of magnitude

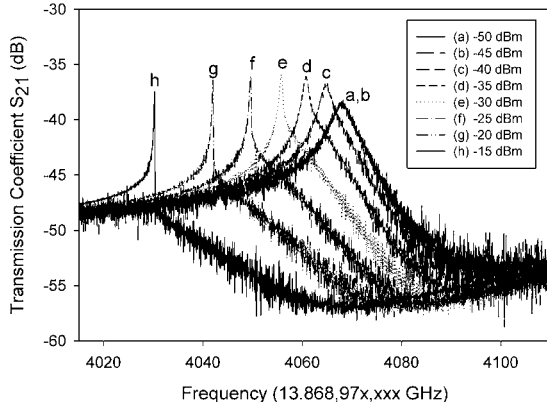


FIG. 1. Network analyzer measurement of the $WGH_{20,0,0}$ mode in transmission at 50 mK. The excitation power was varied in steps of 5 dB from -50 dBm to -15 dBm, and the observed mode frequency was downshifted. The -50 dBm and -45 dBm curves are the highest in frequency and lie on top of one another. The threshold power is defined to be the power incident on the resonator which is sufficient to shift the mode frequency by one bandwidth from the “unperturbed” lowest power measurement

stronger.¹¹ As the network analyzer sweeps in frequency, heating occurs as power is deposited into the sapphire on resonance. The change in permittivity due to temperature causes a shift in the resonant frequency of the mode in the opposite direction to the sweep. The result is an astoundingly narrow, yet artificial linewidth with a sharp threshold. If the frequency was swept in the opposite direction, the mode frequency is shifted in the same direction as the sweep, and an artificially broadened linewidth would be observed. A similar effect in such dielectric resonators has only been observed at optical frequencies in fused silica microspheres.²⁵ It was shown that the “thermal bistability” caused either narrowing or broadening of the line resonance depending on the direction of the frequency sweep during measurement. Examples of optical bistability are numerous in the literature,^{26–28} but are normally attributed to a $\chi^{(3)}$ Kerr nonlinearity, which results in a threshold power for optical bistability that scales like Q^{-2} . Collot *et al.*²⁵ note that for mode Q factors below 10^9 the thermal bistability effect dominates over the Kerr effect due to significantly lower threshold power. For quality factors in the range of 10^9 , the effects can be distinguished by the observed dependence of threshold power on Q . We find an excellent fit using a thermal model (see Eq. (3) and Fig. 4) which has a threshold power that scales like Q^{-1} , showing that the effect is clearly thermal in nature. A measurement of the $WGH_{20,0,0}$ mode was made (see Fig. 1) which shows the observation of this thermal bistability effect in a millikelvin sapphire resonator. A sharp threshold was observed, giving a full width at half maximum linewidth of only 0.00173 Hz, which was strongly dependent on input power. Our experimental apparatus was unable to sweep downwards in frequency but the bistability effect is still observable by varying the sweep speed. Figure 2 shows the effect of the thermal bistability for a range of sweep times. Note that only the resonant peak moves; the longer sweep time results in more time spent per measurement point, depositing more power into the resonator and creating a larger

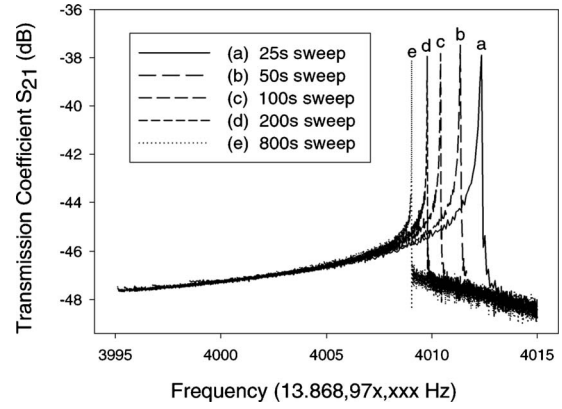


FIG. 2. The $WGH_{20,0,0}$ mode in transmission for varying sweep time. Sweep direction is increasing in frequency in all cases. The linewidth of the mode narrows sharply with sweep time due to temperature dependence of permittivity of the sapphire. The governing equations for the line shape are given in Ref. 26.

apparent frequency shift and linewidth change. As sufficient heat is deposited into the resonator only on resonance, the off-resonance transmission does not depend on sweep time. It is possible to model the threshold power at which bistable behavior becomes apparent. Considering a temperature-dependent fractional frequency shift of the WG mode of interest, $\Delta\nu/\nu = -\alpha\Delta T$, where the temperature coefficient α is experimentally determined, we then expect thermal bistability for a threshold temperature rise of the resonator $\Delta T_{th} = \frac{1}{\alpha} \frac{\Delta\nu}{\nu} = \frac{1}{\alpha Q}$ K. An expression for the threshold power required to achieve this bistability is given by²⁵

$$P_{th} = \frac{C_p \rho V_{eff} \Delta T_{th}}{\tau_T}, \quad (1)$$

where C_p is the heat capacity of sapphire, ρ is its density [4.0 g/cm^3 (Ref. 29)], τ_T the characteristic heat diffusion time constant, and V_{eff} the effective volume occupied by the whispering-gallery mode. The heat-diffusion time constant in turn may be expressed as

$$\tau_T = \frac{lmC_p}{Ak}, \quad (2)$$

where l and A are the length and cross-sectional area of the sapphire segment, m is the mass of the sapphire, and k the thermal conductivity.³⁰ Finally, an expression (independent of the heat capacity and thermal time constant) is derived by combining Eqs. (1) and (2)

$$P_{th} = \frac{Ak}{l\alpha Q} \frac{m_{eff}}{m}, \quad (3)$$

where m_{eff} is the mass of the effective volume occupied by the WG mode. The expression for the threshold power is now clearly only a function of the thermal coefficient α , Q factor, and thermal conductivity of the sapphire, as well as its dimensions. The thermal conductivity k was estimated by fitting an approximate T^3 power law to extrapolate below 1 K from the data for sapphire in Touloukian *et al.*,³¹ giving $k = 0.0397^{2.8924} \text{ W cm}^{-1} \text{ K}^{-1}$. The thermal time constant of

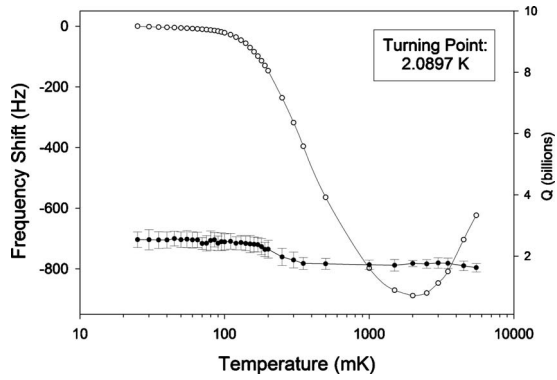


FIG. 3. Temperature dependence of Q factor (shaded circles) and frequency (empty circles) for the 20th azimuthal order WG mode. Note that due to paramagnetic impurities in the sapphire, df/dT is annulled at 2.0897 K. The Q factor remains approximately constant over a wide range of temperature.

sapphire remains similar to that at liquid-helium temperature because the heat capacity follows a similar cubic law to the thermal conductivity, leaving the ratio unchanged [Eq. (2)]. However, the threshold for bistability is substantially lowered with respect to liquid-helium temperature due to the reduction in thermal conductivity of the sapphire.

To experimentally determine the thermal coefficient α , frequency measurements of several whispering-gallery modes were made over a range of temperatures from 25 mK to 5.5 K. The modes examined were fundamental quasi-transverse magnetic modes $WGH_{14,0,0}$, $WGH_{19,0,0}$, and $WGH_{20,0,0}$. The modes were excited using a vector network analyzer at low power, typically -45 dBm. In this way, saturation of residual paramagnetic spins in the sapphire was avoided. The temperature of the resonator was controlled at a number of points between 25–5500 mK using a Lakeshore Model 370 AC Resistance Bridge, and custom data acquisition software recorded the temperature, Q factor, and frequency of the modes in transmission. The base temperature of the dilution refrigerator was 23 mK and temperature control was stable to within several millikelvin. The temperature dependence of mode frequency was mapped to produce plots such as Fig. 3 and several temperatures were chosen to measure the threshold power at which thermal bistability became apparent. The temperatures were chosen to reflect a range of values for the thermal coefficient α , ranging from nominally zero near the frequency-temperature turnover point, to a maximum at the largest slope. As previously, we define the threshold power to be the power incident on the resonator which is sufficient to shift the mode frequency by one bandwidth from the unperturbed low-power measurement. Equation (3) is then used to calculate the theoretical threshold power. The experimentally determined thermal coefficients are summarized in Table I and a particular example of the measured and calculated threshold power is given in Fig. 4 for $WGH_{20,0,0}$.

Clearly, operation at the frequency temperature turning point is advantageous as the thermal coefficient α approaches zero and the threshold power required for bistability approaches infinity. Temperature turning points have been observed with no bistability at input powers up to 20 dBm

TABLE I. Measured parameters for the thermal coefficient and Q .

m	T (mK)	Q	α
14	100	7.84×10^8	-6.66×10^{-9}
	800	1.7×10^9	-1.3×10^{-11}
19	100	6.17×10^8	-6.85×10^{-8}
	440	5.40×10^8	-1.10×10^{-7}
	2260	5.85×10^8	-1.60×10^{-11}
20	200	2.21×10^9	-1.19×10^{-7}
	630	1.72×10^9	-3.26×10^{-8}
	2100	1.76×10^9	-5.85×10^{-11}

from 4–9 K in similar sapphire resonators, and are caused by residual paramagnetic impurities such as Ti^{3+} , Cr^{3+} , Mo^{3+} , V^{3+} , Mn^{3+} , and Ni^{3+} present at concentrations of parts-per-billion to parts-per-million. The opposite sign effects of temperature-dependent Curie law paramagnetic susceptibility and temperature dependence of permittivity^{32–36} cause a turnover in the frequency-temperature dependence. Operating at this turning point or “magic temperature” allows frequency fluctuations due to temperature instability to be annulled to first order, and has been crucial to achieve state-of-the-art short term fractional frequency stability in CSOs in the past.^{9,20,32} Our results are the first observation of temperature turning points below the boiling point of liquid helium. Table II lists the magic temperatures (turning points) measured for a range of WG modes. Operation of the WHIGMO at a millikelvin magic temperature rather than its current ≈ 8 K would have the benefit of reduced thermal noise floor of the maser, with potential operation at the quantum limit. Operation at a millikelvin turning point, where the thermal coefficient α is vanishing, would minimize the effects from the considerable heating due to the large (>10 dBm) input power required to saturate the pump transition of the maser. This is similarly advantageous for CSOs (Ref. 20) which typically circulate large amounts of power through the sapphire resonator, at least several milliwatt,

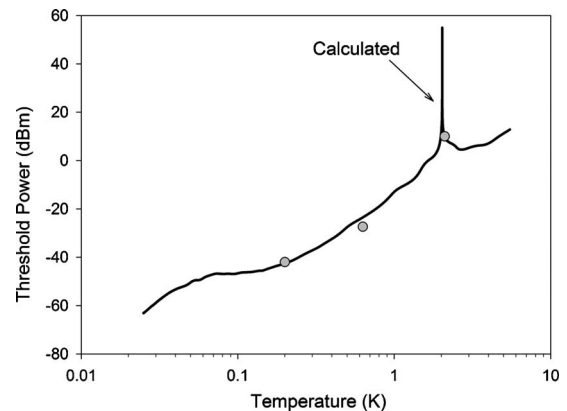


FIG. 4. Predicted threshold power [using Eq. (3)] as a function of temperature for $WGH_{20,0,0}$. Shaded circles are the measured threshold values for 200, 630, and 2100 mK.

TABLE II. Measured “magic temperatures” for a range of quasitransverse magnetic WG modes. Several modes close to the Fe³⁺ center frequency exhibited strong distortion and could not be accurately tracked to determine the turning point. The $m=17$ mode required large power to excite and could not be measured below 80 mK due to heating effects.

m	Magic temperature (mK)
13	89.75
14	96.25
15	Not trackable
16	Not trackable
17	Possible turnover below 80 mK
18	2749.35
19	2280.30
20	2089.75

while the cooling power at base temperature of a dilution refrigerator is only on the order of several hundred μW . Additionally, high-power operation of quantum limited transducers could be attained at these temperatures.

In summary, we report the characterization of a single-crystal sapphire resonator at temperatures more than an order of magnitude lower than previously achieved, the measurement of thermal bistability in a microwave sapphire resonator at these temperatures, and the observation of millikelvin

frequency-temperature turning points. We give a model for the thermal bistability threshold power and show that it is closely dependent on the material properties of the sapphire resonator. We propose several reasons the effect has not been previously observed in this system. Typically the CSO/WHIGMO is operated very close to a frequency-temperature turning point where the temperature coefficient α is small, and the threshold power for bistability becomes significantly larger than normal operational power levels. In the experiments reported in this paper, the resonator was operated at low temperature, far from a turning point where the temperature coefficient was large, leading to a lower and readily observable threshold power. Frequency-temperature turning points as low as tens of millikelvins were observed for WG modes in the resonator and we show that the thermal bistability effect can be suppressed by operating at these “magic temperatures.” Additionally, mode Q factors remained high and were comparable to their usual values at higher temperature, ruling out the existence of extra loss mechanisms in sapphire in the millikelvin regime. We conclude that single-crystal sapphire is an excellent candidate for both clock applications and quantum metrology of macroscopic systems at temperatures approaching absolute zero.

This work was supported in part by Australian Research Council Grants No. FL0992016, No. DP0986932, and No. FF0776191 and a University of Western Australia collaboration grant.

*creedon@physics.uwa.edu.au

- ¹T. Rocheleau, T. Ndukum, C. Macklin, J. B. Hertzberg, A. A. Clerk, and K. C. Schwab, *Nature (London)* **463**, 72 (2010).
- ²A. O’Connell, M. Hofheinz, M. Ansmann, R. C. Bialczak, M. Lenander, E. Lucero, M. Neeley, D. Sank, H. Wang, M. Weides, J. Wenner, J. M. Martinis, and A. N. Cleland, *Nature (London)* **464**, 697 (2010).
- ³M. Hofheinz, H. Wang, M. Ansmann, R. C. Bialczak, E. Lucero, M. Neeley, A. D. O’Connell, D. Sank, J. Wenner, J. M. Martinis, and A. N. Cleland, *Nature (London)* **459**, 546 (2009).
- ⁴M. Hofheinz, E. Weig, M. Ansmann, R. C. Bialczak, E. Lucero, M. Neeley, A. D. O’Connell, H. Wang, J. M. Martinis, and A. N. Cleland, *Nature (London)* **454**, 310 (2008).
- ⁵K. Osborn, J. Strong, A. Sirois, and R. Simmonds, *IEEE Trans. Appl. Supercond.* **17**, 166 (2007).
- ⁶M. Sandberg, C. Wilson, F. Persson, T. Bauch, G. Johansson, V. Shumeiko, T. Duty, and P. Delsing, *Appl. Phys. Lett.* **92**, 203501 (2008).
- ⁷M. Castellanos-Beltran and K. Lehnert, *Appl. Phys. Lett.* **91**, 083509 (2007).
- ⁸A. Mann, in *Frequency Measurement and Control: Advanced Techniques and Future Trends*, edited by A. Luiten (Springer, Berlin, 2001), pp. 37–66.
- ⁹J. G. Hartnett, C. R. Locke, E. N. Ivanov, M. E. Tobar, and P. L. Stanwix, *Appl. Phys. Lett.* **89**, 203513 (2006).
- ¹⁰C. R. Locke, M. E. Tobar, and E. N. Ivanov, *Rev. Sci. Instrum.* **71**, 2737 (2000).
- ¹¹V. Braginsky, V. Mitrofanov, and V. Panov, *Systems with Small Dissipation* (University of Chicago Press, Chicago, 1985).
- ¹²J. Krupka, K. Derzakowski, A. Abramowicz, M. E. Tobar, and R. G. Geyer, *IEEE Trans. Microwave Theory Tech.* **47**, 752 (1999).
- ¹³J. Krupka, K. Derzakowski, M. E. Tobar, and R. G. Geyer, *Meas. Sci. Technol.* **10**, 387 (1999).
- ¹⁴C. R. Locke, M. E. Tobar, and E. N. Ivanov, *Class. Quantum Grav.* **19**, 1877 (2002).
- ¹⁵M. E. Tobar, *Physica B: Condens. Matter* **280**, 520 (2000).
- ¹⁶C. R. Locke and M. E. Tobar, *Meas. Sci. Technol.* **15**, 2145 (2004).
- ¹⁷M. E. Tobar, E. N. Ivanov, D. K. L. Oi, B. D. Cuthbertson, and D. G. Blair, *Appl. Phys. B: Lasers Opt.* **64**, 153 (1997).
- ¹⁸B. D. Cuthbertson, M. E. Tobar, E. N. Ivanov, and D. G. Blair, *Rev. Sci. Instrum.* **67**, 2435 (1996).
- ¹⁹M. E. Tobar and A. G. Mann, *IEEE Trans. Microwave Theory Tech.* **39**, 2077 (1991).
- ²⁰C. R. Locke, E. N. Ivanov, J. G. Hartnett, P. L. Stanwix, and M. E. Tobar, *Rev. Sci. Instrum.* **79**, 051301 (2008).
- ²¹P. Y. Bourgeois, N. Bazin, Y. Kersalé, V. Giordano, M. E. Tobar, and M. Oxborrow, *Appl. Phys. Lett.* **87**, 224104 (2005).
- ²²K. Benmessai, D. L. Creedon, M. E. Tobar, P. Y. Bourgeois, Y. Kersale, and V. Giordano, *Phys. Rev. Lett.* **100**, 233901 (2008).
- ²³D. L. Creedon, K. Benmessai, M. E. Tobar, J. G. Hartnett, P.-Y. Bourgeois, Y. Kersale, J.-M. Le Floch, and V. Giordano, *IEEE*

- [Trans. Ultrason. Ferroelectr. Freq. Control](#) **57**, 641 (2010).
- ²⁴K. Benmessai, [Electron. Lett.](#) **43**, 1436 (2007).
- ²⁵L. Collot, V. Lefèvre-Seguin, M. Brune, J. Raimond, and S. Haroche, [Europhys. Lett.](#) **23**, 327 (1993).
- ²⁶T. Carmon, L. Yang, and K. Vahala, [Opt. Express](#) **12**, 4742 (2004).
- ²⁷V. B. Braginsky, M. L. Gorodetsky, and V. S. Ilchenko, [Phys. Lett. A](#) **137**, 393 (1989).
- ²⁸H. Rokhsari, S. M. Spillane, and K. Vahala, [Appl. Phys. Lett.](#) **85**, 3029 (2004).
- ²⁹*Handbook of Chemistry and Physics*, 55th ed., edited by R. Weast (CRC Press, Cleveland, OH, 1974).
- ³⁰M. Tobar, E. Ivanov, R. Woode, and J. Searls, Proceedings of the 1994 IEEE International Frequency Control Symposium, 1994 (unpublished), pp. 433–440.
- ³¹Y. Touloukian, R. W. Powell, C. Y. Ho, P. G. Klemens, and E. H. Buyco, *Thermophysical Properties of Matter* (IFI/Plenum, New York, 1970), Vols. 2 and 4.
- ³²G. J. Dick, D. G. Santiago, and R. T. Wang, [IEEE Trans. Ultrason. Ferroelectr. Freq. Control](#) **42**, 812 (1995).
- ³³S. K. Jones, D. G. Blair, and M. J. Buckingham, [Electron. Lett.](#) **24**, 346 (1988).
- ³⁴A. G. Mann, A. J. Giles, D. G. Blair, and M. J. Buckingham, [J. Phys. D](#) **25**, 1105 (1992).
- ³⁵J. G. Hartnett, M. E. Tobar, A. G. Mann, E. N. Ivanov, J. Krupka, and R. Geyer, [IEEE Trans. Ultrason. Ferroelectr. Freq. Control](#) **46**, 993 (1999).
- ³⁶M. E. Tobar, J. Krupka, E. N. Ivanov, and R. A. Woode, [J. Phys. D](#) **30**, 2770 (1997).